

## Synthesis of Fe/C Nanocomposites by Decomposition of Iron Pentacarbonyl in Electric Arc Discharge

ALEXANDER V. OKOTRUB<sup>1</sup>, VLADIMIR L. KUZNETSOV<sup>2</sup>, ALEXANDRA SHARAYA<sup>3</sup>, YURIY V. BUTENKO<sup>2</sup>, ANDREY L. CHUVILIN<sup>2</sup>, YURIY V. SHUBIN<sup>1</sup>, VLADIMIR A. VARNEK<sup>1</sup>, OLIVER KLEIN<sup>3</sup> and HUBERT PASCARD<sup>3</sup>

<sup>1</sup>*Nikolaev Institute of Inorganic Chemistry, Siberian Branch of the Russian Academy of Sciences, Pr. Akademika Lavrentyeva 3, Novosibirsk 630090 (Russia)*

*E-mail: spectrum@che.nsk.su*

<sup>2</sup>*Boreskov Institute of Catalysis, Siberian Branch of the Russian Academy of Sciences, Pr. Akademika Lavrentyeva 5, Novosibirsk 630090 (Russia)*

<sup>3</sup>*Ecole Polytechnique, 91128, Palaiseau Cedex, Paris (France)*

### Abstract

A fibrous material composed of filamentary crystals of iron carbide Fe<sub>3</sub>C or metal iron encapsulated in graphite shells is synthesized. Combined investigation of the structure of the obtained material is performed by means of electron microscopy, powder X-ray diffractometry and Mössbauer spectroscopy. It is discovered that current-voltage characteristics of auto-emission properties of nanoparticles differ from the properties of pure carbon nano-tubes, which is explained by different adsorption characteristics of these materials.

### INTRODUCTION

Composite ultrafine particles of metal iron, its oxides and carbides attract substantial attention in connection with the outlooks for the creation of new magnetic materials. The use of various synthesis methods, changes in the parameters of particle formation allow one to affect their structure and properties. Methods of gas-phase decomposition of organometallic compounds are widely used to synthesize ultrafine iron particles [1]. Evaporation of graphite with metals under the arc discharge conditions, which are extremely non-uniform with respect to temperature and pressure, in combination with the flux of carbon atoms, allows synthesizing various metal and carbide nanoparticles based on containing transition and rare-earth metals. Kretschmer-type reactor with composite anode, developed for the synthesis of fullerenes and carbon nano-tubes, are usually used for this purpose. In these reactors, both electrodes are made of graphite; metal is introduced into one of them in the form of a powder [2, 3].

The nanoparticles formed have different morphology. At present the most substantial attention is attracted to the study of the influence of the effect of metal nature on the formation of carbon nano-tubes [4–6]. However, evaporation and condensation of metals in the arc lead also to the synthesis of ball-shaped particles coated with several layers of graphite. Two types of metal-containing particles without carbon layer were obtained by the evaporation of iron electrode in the direct-current arc plasma. The particles of the first type were very small (~15–30 nm); they were composed of iron carbide [7]. The particles of the second type were multilayered structures composed of  $\alpha$ -Fe, Fe<sub>3</sub>O<sub>4</sub> and FeO(OH), with the size up to 100 nm. In the case of synthesis in the arc of alternate current, particles covered with carbon layer are obtained. The carbon layer protects them from oxidation in the air [8]. These particles contain metal carbides or pure metal.

In the present work we introduced iron into electroarc reactor by blowing the vapour of

iron pentacarbonyl with helium into the zone of direct-current electric arc reactor; the structure and some properties of the resulting material were investigated.

## EXPERIMENTAL

Synthesis of iron-carbon particles was performed in the set-up of electric arc evaporation of graphite, described in [9, 10]. The reaction volume of the chamber was ~150 l. The lower negative electrode was made of graphite 60 mm in diameter. The mobile upper electrode (anode) was composed of 7 standard graphite electrodes of C3 grade, 6 mm in diameter. The length of electrodes was 200 mm. Evaporation of anode was performed for ~15–20 min at the voltage between electrodes of ~35–40 V and the current of ~600 A.

Before using,  $\text{Fe}(\text{CO})_5$  was purified by vacuum distillation. The introduction of iron carbonyl was performed by passing helium flow (1 l/min) through a bubbler with the liquid carbonyl heated to 50 °C. The gas temperature in the chamber was maintained at ~350 °C during evaporation. The nozzle of the inlet tube was cooled with water and protected from irradiation with a screen made of tungsten foil. About 15 g of iron carbonyl was admitted into the chamber during one experiment. A constant He pressure of 0.5 atm was maintained during the synthesis. Mass spectrometric monitoring of the composition of the gas phase was performed with MX-7304 mass spectrometer. As  $\text{Fe}(\text{CO})_5$  was added, permanent increase in the concentration of  $\text{CO}^+$  ion was observed, which was the evidence of the accumulation of CO in the gas phase.

X-ray diffraction measurements were performed with DRON-Roentgen-Master-4 diffractometer ( $\text{CuK}_\alpha$  radiation, graphite monochromator, stepwise recording). Mössbauer spectra of the samples 1 and 2 were measured at 295 K using NP-610 spectrometer with  $^{57}\text{Co}(\text{Rh})$  source. Electron microscopic investigation was performed using JEM-2010 and JEOL 4000FX microscopes.

The field emission of the sample was measured in the diode mode in the vacuum of  $\sim 10^{-4}$  Pa and room temperature. Pressed sample

with the surface area of 1 mm<sup>2</sup> was fixed on the surface of nickel cathode. The distance between cathode and anode was 500  $\mu\text{m}$ . The measurement of tunneling current was performed every 0.2 s with the saw-tooth voltage up to 1500 V with the frequency of 0.01–0.1 Hz.

## STRUCTURE AND PROPERTIES OF THE OBTAINED MATERIALS

Electric arc evaporation of pure graphite rods in helium leads to the formation of carbon buildup incrustation containing multilayered nano-tubes, and fullerene-containing ash on the walls of the reactor [9]. An introduction of  $\text{Fe}(\text{CO})_5$  vapour into the system leads to the formation of a fibrous material which is deposited directly near the place of the admission of iron carbonyl vapour.

### *Electron microscopic investigation*

Electron microscopic images of the obtained material show that it is composed mainly of filamentary crystals of iron or iron carbide coated with several graphite layers. A micrograph shown in Fig. 1, *a* allows considering the particles' morphology. One can see that winding filaments have relatively small number of branching. The diameter of filaments is ~10–200 nm. It should be noted that the change in their thickness accounts for 20–40 % of mean thickness. Sometimes, the inner metal part gets broken into separate metal particles bound by multilayered carbon nano-tubes. In addition, metal particles of spherical and quasi-spherical shapes encapsulated in carbon layers were detected.

The investigation of the chemical composition of individual particles with the help of energy-dispersion X-ray analysis (EDX) stated the presence of two elements: iron and carbon. An EDX spectrum obtained using an electron beam 34 nm in size is shown in Fig. 1, *b*. One can see peaks of Fe  $K_\alpha$  and  $K_\beta$ . Copper lines relate to the material of the network used as a grid. Carbon peak is also observed in the spectrum; it can correspond to the amorphous carbon of the substrate, outer carbon layer which is on the surface of metal crys-

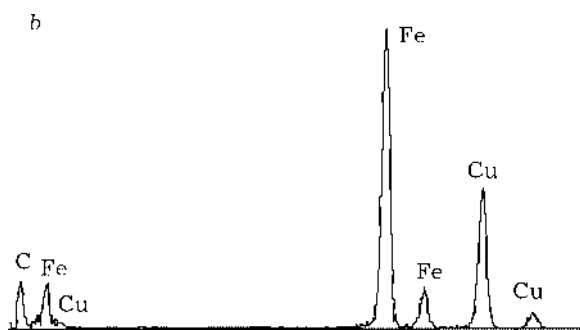
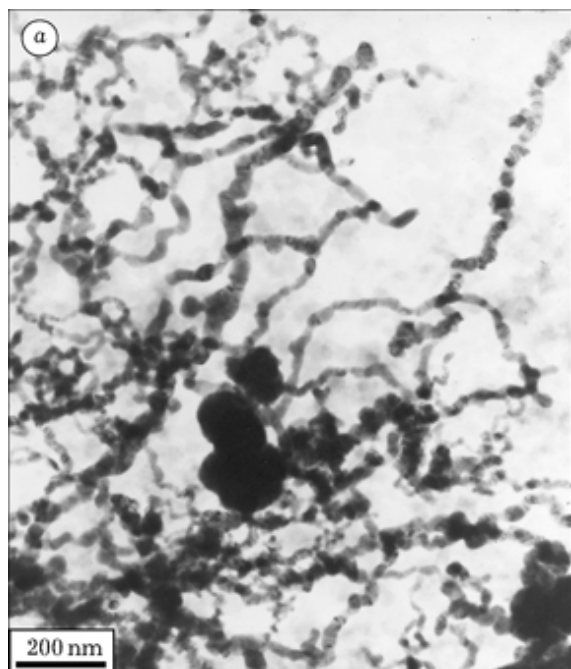


Fig. 1. Plan view micrograph of filamentary crystals synthesized in arc discharge (a) and the data of energy dispersion X-ray analysis demonstrating the composition of nanocrystal (b).

tals, and Fe-C compounds. The spectrum of Fe  $L_{\alpha}$  coincides in energy with the  $K_{\alpha}$  spectrum of oxygen, which is usually observed in most EDX spectra. Because of this, one may conclude on the basis of EDX results that the observed crystallites are composed of pure Fe or of its carbide or oxide.

#### X-ray phase analysis

According to XPA data, the sample obtained contains cementite ( $\text{Fe}_3\text{C}$ ) and  $\alpha$ -modification of iron in comparable amounts (Fig. 2). Iron lines are noticeably broadened due to small size of crystallites. Mean coherent length calculated using the integral width of (002) reflection is 120 Å the size of crystallites in ce-

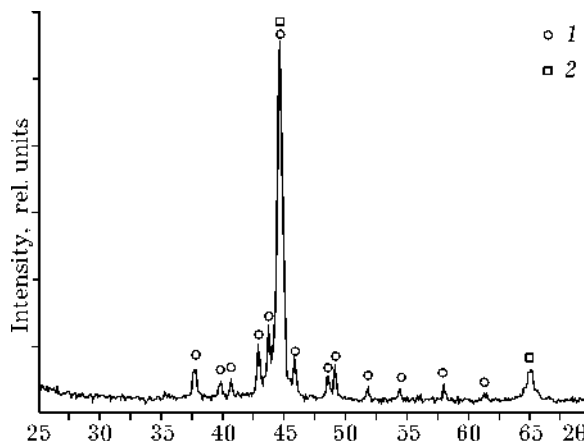


Fig. 2. X-ray diffraction patterns of the pressed sample of material containing nano-filaments: 1 - lines corresponding to the reflection of crystallites of carbide  $\text{Fe}_3\text{C}$ ; 2 - lines of  $\alpha$ -Fe.

mentite phase is about 500 Å. In addition, weak lines of iron oxide  $\text{Fe}_2\text{O}_3$  are observed in the diffraction patterns.

#### Mössbauer spectroscopy

The Mössbauer spectrum of the powdered sample is shown in Fig. 3. The spectrum is a superposition of two magnetic sextets; for one of them, magnetic field on iron nuclei is  $H_{\text{ef}} = (330 \pm 2)$  kOe, and for another  $H_{\text{ef}} = (208 \pm 2)$  kOe. The former sextet relates to  $\alpha$ -Fe, the latter to carbide  $\text{Fe}_3\text{C}$ . Relative content of iron atoms in this sample, estimated using line intensities, is 40 and 60 %, respectively.

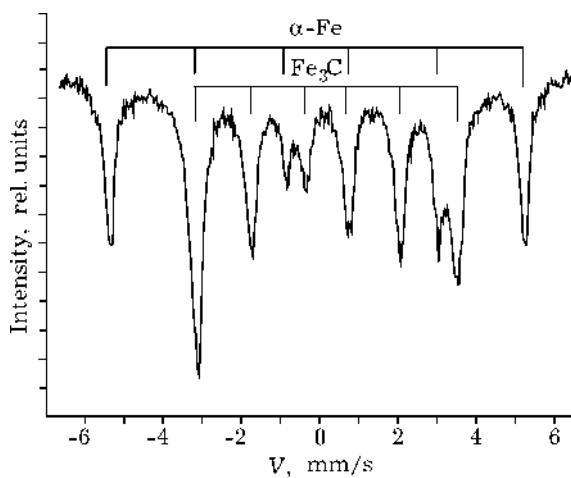


Fig. 3. Mössbauer spectra of the synthesized sample and its decomposition into the components  $\alpha$ -Fe and  $\text{Fe}_3\text{C}$ .

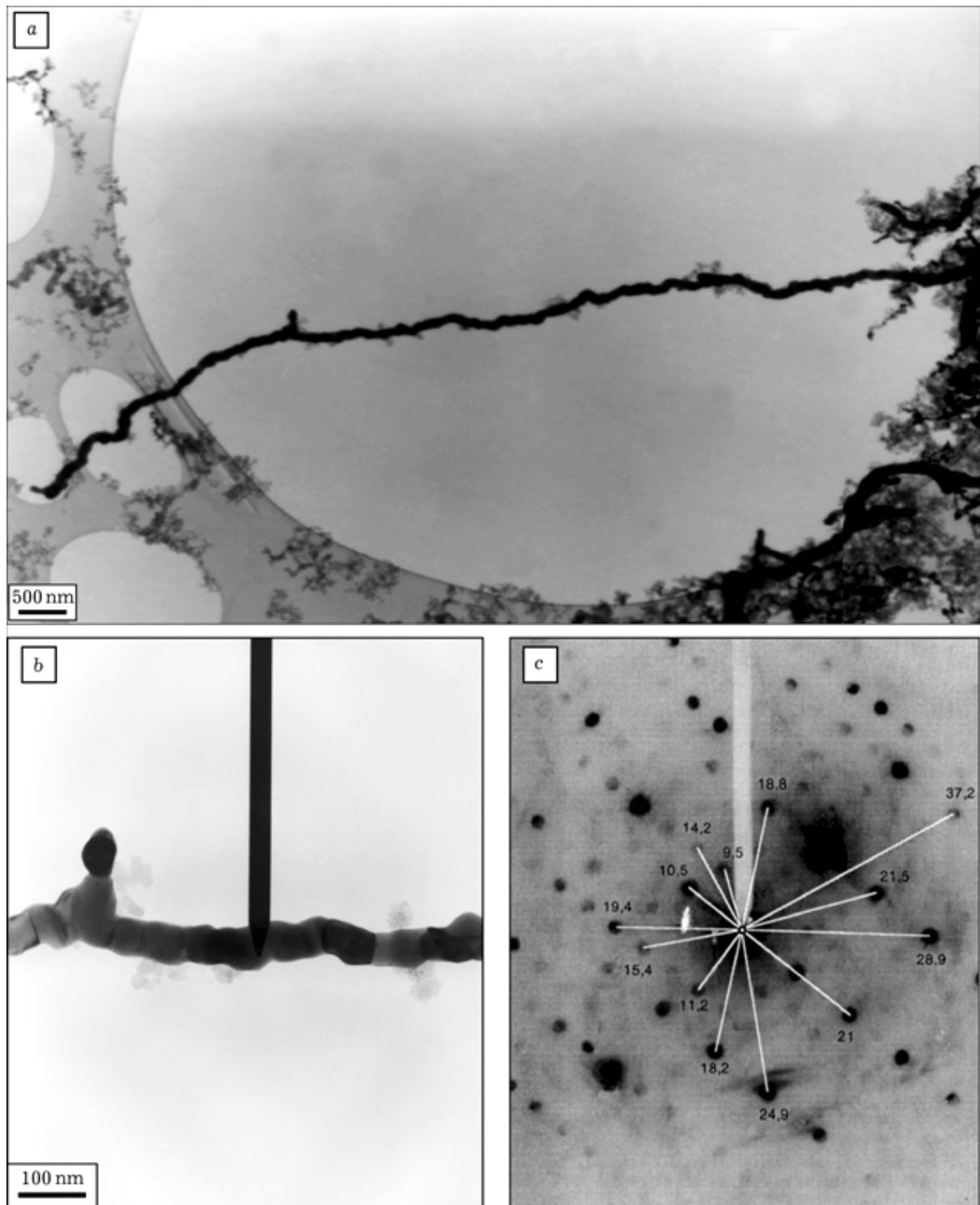


Fig. 4. Plan view micrograph of filamentary crystal (a), crystal region on which microdiffraction was measured (b), and microdiffraction indicating the presence of  $\text{Fe}_3\text{C}$  phase (c).

### Microdiffraction and spectroscopy of energy losses

Methods of electron microscopy allow one to investigate crystal structure using the diffraction of electron beam passing through a nanoparticle. The diffraction patterns of filamentary crystal are shown in Fig. 4. Single crystal filament successfully got right at the hole of the polymeric film supporting the sample (see Fig. 4, *a*). The filament is composed of monocrystallites 30 nm in diameter and about 50 nm long. These crystallites can be rather well distinguished in Fig. 4, *b*, which presents with high magnification a region in which electron diffraction measurements were performed. The set of diffraction points and distances shown in Fig. 4, *c* confirms that these crystallites have the structure of carbide  $\text{Fe}_3\text{C}$ .

One can see in high-resolution micrographs (Fig. 5, *a*) that iron-containing crystallites can be encapsulated in graphite layers; the number of these layers can be from one or three to several tens. In addition, the thickness of graphite layer can change substantially over the length of one crystal.

Chemical composition of the encapsulated crystals was investigated using electron energy loss spectroscopy (EELS). We obtained the data on spatial distribution of different elements in the crystal volume and discovered the structures of two types. The first one is represented by iron carbide crystals encapsulated in carbon layer about 10 nm thick (see Fig. 5, *b*). Other nanocrystals contain the oxide layer of 5 to 12 nm thick, non-uniformly distributed around the central crystal composed of pure iron (see Fig. 5, *c*).

### Measurement of electron autoemission

The features of the structure of whiskers and filamentary crystals composed of iron determine a set of their unusual properties making their use promising for the creation of high-strength composite materials, permanent magnets, *etc.* One of these properties, which is due to the features of morphology and electron structure of the synthesized material, is autoemission of electrons at low electric field strength.

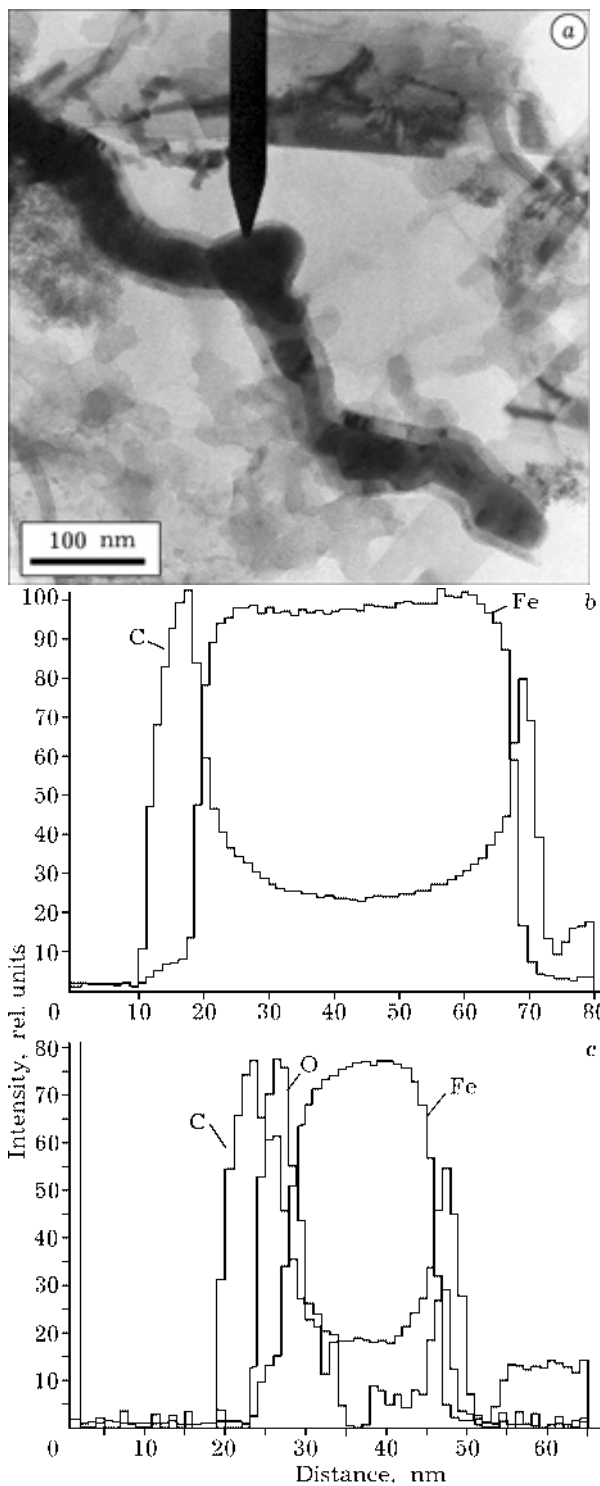


Fig. 5. Micrograph of iron crystal encapsulated into graphite layers (*a*), and profiles of the distribution of elements C, Fe, O for two different crystals (*b*, *c*).

Current-voltage characteristics (CVC) of the field emission of a pressed sample with the area of  $1 \text{ mm}^2$  is shown in Fig. 6, *a*. The appearance of noticeable (more than  $1 \mu\text{A}$ ) tunneling current occurs at the electric field

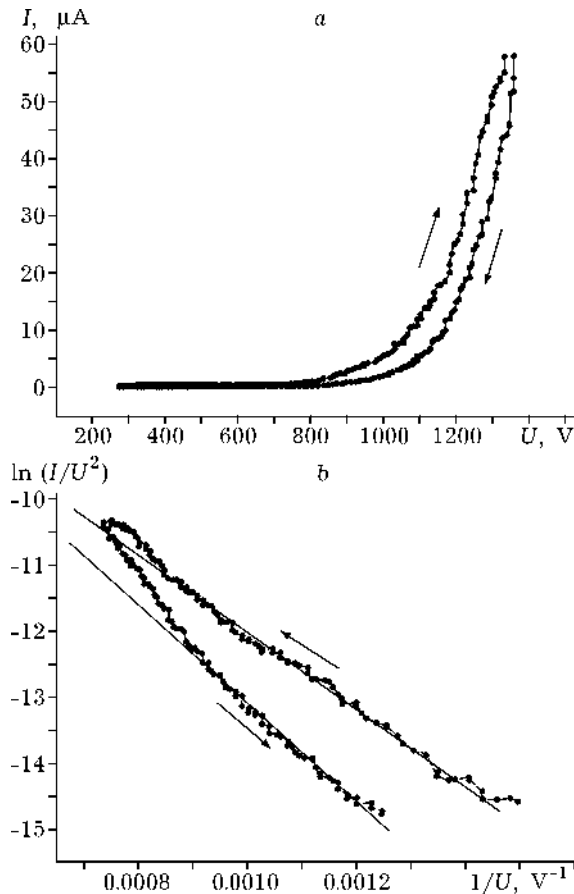


Fig. 6. Dependence of the current of field emission of filamentary particles on voltage (a), and its representation in Fowler - Nordheim coordinates (b).

strength of  $\sim 1.4$  V/ $\mu\text{m}$ . Maximal current in the field of  $\sim 2$  V/ $\mu\text{m}$  was  $\sim 100$   $\mu\text{A}$ . These data confirm high emission ability of metal and carbide filaments and outlook of using this material for manufacturing cool cathodes. When measuring CVC in the modes of increasing and decreasing voltage, we discovered hysteresis of the emissive properties of the film. In the inverse mode, electron emission disappears at higher electric field strength (1.5 V/ $\mu\text{m}$ ). Previously, it was demonstrated [11] that such a change in emissive properties of nano-tubes can be explained by the effects in terms of adsorption and desorption of the residual gases during electron autoemission. Investigation of the optical emission spectrum of carbon nano-tubes during field emission shows that it is in consistency with the distribution of the black-body radiation [12]. Thus, at a large emission current, temperature of tubes raises to 600  $^{\circ}\text{C}$  and above. At this temperature, sub-

stantial desorption of the absorbed gases occurs. It was interesting to compare emissive characteristics of the obtained carbon-iron samples and of pure carbon-containing systems. As we have already mentioned, carbon nano-tubes are among the most promising materials for the development of cold cathodes. The observed changes in the CVC of pure carbon nano-tubes [11] are much smaller than those exhibited by our material. It may be assumed that the synthesized material possesses higher sorption ability than pure nano-tubes.

Fowler - Nordheim characteristics for the ascending and descending branches only weakly deviate from the theoretical linear dependence (see Fig. 6, b). However, their slopes differ substantially. From the viewpoint of autoelectron emission, the character of changes in emissive properties of the substance under investigation in the mode of decreasing electric field strength is equivalent to an increase in work function. The possibility of high emissive properties of the synthesized material being determined by graphite shells comprising the outer layers of nanoparticles cannot be excluded.

## CONCLUSIONS

The formation of large number of metal-containing filaments with a diameter from 10 to 100 nm on adding iron carbonyl  $\text{Fe}(\text{CO})_5$  into the gas phase of the electroarc graphite evaporation reactor was discovered. A substantial part of these particles is coated with carbon shells. It is demonstrated by means of X-ray diffraction and Mössbauer spectroscopy that the sample contains two main forms:  $\alpha$ -Fe and  $\text{Fe}_3\text{C}$ , as well as a small amount of  $\text{Fe}_2\text{O}_3$ . The data of microdiffraction confirm that the particles having no graphite shell are  $\text{Fe}_3\text{C}$  crystallites. Nanoparticles coated with graphite shells differ in structure and composition. Some of the encapsulated metal particles are coated with oxide layer up to 15 nm thick. It may be assumed that the oxide layer produce not due to passivation but during the formation of these particles, because carbon layers prevent metal oxidation. At the same time, the

major part of encapsulated crystals does not contain oxygen and is most likely composed of Fe<sub>3</sub>C carbide, which possesses high stability toward oxidation. The synthesized material, composed of nano-filaments, possess special electron properties. In particular, it was discovered that its autoemission characteristics are not worse than those of carbon nanotubes and diamond films. A feature of the current-voltage characteristics of these nanoparticles is the occurrence of hysteresis, which is due to the adsorption of residual gases. An assumption is put forward that the sorption properties of filaments are higher than those of carbon nano-tubes.

### Acknowledgements

The investigation has been supported by INTAS (Grant No. 00-237, 01-254) and RFBR (Grant No. 00-03-32510).

### REFERENCES

- 1 V. G. Syrkin, CVD-method. Chemical vapour phase metallization. Khimicheskaya parofaznaya metallizatsiya, Nauka, Moscow, 2000.
- 2 J. Jiao, S. Seraphin, X. Wang and J. Whitters, *J. Appl. Phys.*, 80, 1 (1996) 103.
- 3 M. E. McHenri, S. A. Majetich, J. O. Artman *et al.*, *Phys. Rev. B.*, 49, 16 (1994) 11358.
- 4 B. C. Satishkumar, A. Govindaraj, C. N. R. Rao, *Chem. Phys. Lett.*, 307 (1999) 158.
- 5 K. Hernadi, A. Fonseca, J. B. Nagy *et al.*, *Carbon*, 34 (1996) 1249.
- 6 A. M. Valiente, P. N. Lopez, I. R. Ramos *et al.*, *Ibid.*, 38 (2000) 2003.
- 7 M. Hanson, C. Johanson, M. S. Pedersen and S. Morup, *J. Phys.: Condens. Matter.*, 7 (1995) 9269.
- 8 G. L. Zhang, F. Ambe, E. H. du Marchie Van Voorthusen *et al.*, *J. Appl. Phys.*, 80, 1 (1996) 579.
- 9 A. V. Okotrub, Yu. V. Shevtsov, L. I. Nasonova *et al.*, *Pribory i tekhnika experimenta*, 1 (1995) 193.
- 10 A. V. Okotrub, Yu. V. Shevtsov, L. I. Nasonova *et al.*, *Neorgan. materialy*, 32, 8 (1996) 974.
- 11 K. A. Dean, B. R. Chalamala, *Appl. Phys. Lett.*, 76, 3 (2000) 375.
- 12 J.-M. Bonard, T. Stockli, F. Maier *et al.*, *Phys. Rev. Lett.*, 81, 7 (1998) 1441.